



JGR Atmospheres

RESEARCH ARTICLE

10.1029/2023JD039576

Key Points:

- Threshold velocities for wind erosion increase with increasing soil salinity because salts induce the formation of a soil crust
- Crust formation and aggregation can delay dust emission from soil surfaces even under low salinity conditions
- Salts are preferentially emitted and amplified in airborne dust

Supporting Information:

Supporting Information may be found in the online version of this article.

Correspondence to:

S. Ravi, sravi@temple.edu

Citation:

Khatei, G., Rinaldo, T., Van Pelt, R. S., D'Odorico, P., & Ravi, S. (2024). Wind erodibility and particulate matter emissions of salt-affected soils: The case of dry soils in a low humidity atmosphere. *Journal of Geophysical Research:*Atmospheres, 129, e2023JD039576. https://doi.org/10.1029/2023JD039576

Received 2 JUL 2023 Accepted 17 DEC 2023

Author Contributions:

Conceptualization: R. Scott Van Pelt, Paolo D'Odorico, Sujith Ravi Data curation: Ganesh Khatei, Tobia Rinaldo

Formal analysis: Ganesh Khatei, Tobia Rinaldo

Funding acquisition: R. Scott Van Pelt, Paolo D'Odorico, Sujith Ravi Investigation: Ganesh Khatei, Tobia Rinaldo, R. Scott Van Pelt, Paolo D'Odorico, Sujith Ravi Methodology: Ganesh Khatei, Tobia Rinaldo, R. Scott Van Pelt, Paolo D'Odorico, Sujith Ravi Project Administration: Paolo

P'Odorico, Sujith Ravi
Resources: R. Scott Van Pelt, Sujith Ravi
Supervision: R. Scott Van Pelt, Paolo
D'Odorico, Sujith Ravi

Visualization: Ganesh Khatei, Tobia Rinaldo, Sujith Ravi

© 2024. American Geophysical Union. All Rights Reserved.

Wind Erodibility and Particulate Matter Emissions of Salt-Affected Soils: The Case of Dry Soils in a Low Humidity Atmosphere

Ganesh Khatei¹, Tobia Rinaldo², R. Scott Van Pelt³, Paolo D'Odorico², and Sujith Ravi¹

¹Department of Earth & Environmental Science, Temple University, Philadelphia, PA, USA, ²Department of Environmental Science, Policy, and Management, University of California, Berkeley, CA, USA, ³Wind Erosion and Water Conservation Research, USDA-ARS, Big Spring, TX, USA

Abstract Arid and semiarid ecosystems around the world are often prone to both soil salinization and accelerated soil erosion by wind. Soil salinization, the accumulation of salts in the shallow portions of the soil profile, is known for its ability to decreases soil fertility and inhibit plant growth. However, the effect of salts on soil erodibility by wind and the associated dust emissions in the early stages of soil salinization (low salinity conditions) remains poorly understood. Here we use wind tunnel tests to detect the effects of soil salinity on the threshold velocity for wind erosion and dust production in dry soils with different textures treated with salt-enriched water at different concentrations. We find that the threshold velocity for wind erosion increases with soil salinity. We explain this finding as the result of salt-induced (physical) aggregation and soil crust formation, and the increasing strength of surface soil crust with increasing soil salinity, depending on soil texture. Even though saline soils showed resistance to wind erosion in the absence of abraders, the salt crusts were readily ruptured by saltating sand grains resulting in comparable or sometimes even higher particulate matter emissions compared to non-saline soils. Interestingly, the salinity of the emitted dust is found to be significantly higher (5–10 times more) than that of the parent soil, suggesting that soil salts are preferentially emitted, and airborne dust is enriched of salts.

Plain Language Summary In this study we investigated how the use of slightly saline irrigation water may affect soil susceptibility to wind erosion and the dust emission potential of dry soils, and how these processes are affected by the amount of clay in the soil. Results indicated that, even though salinity decreased the susceptibility of soils to wind erosion due to aggregation and crust formation, abrasion by sand particles resulted in the breakdown of saline crusts, leading to emissions comparable or sometimes even higher to those of non-saline soils. The higher salt concentration found in the dust than in the dust-emitting soil suggests that the airborne transport of salts may have important implications for contaminant transport and salinization of downwind areas.

1. Introduction

Salinization is one of the major concerns in many dryland agroecosystems in the United States and around the world, particularly in regions with high evaporative demand, shallow water tables or irrigated with water rich in dissolved solids (Hassani et al., 2020; Rengasamy, 2006; Szabolcs, 1989). Globally, salt-affected areas cover approximately 23% of cultivated agricultural land and 50% of irrigated land (Shahid et al., 2018; Weil & Brady, 2017). Salinization is the process that results in the accumulation of neutral salts—mainly chlorides, and sulfates of calcium, magnesium, potassium and sodium—in the surface soil. Salt accumulation in the root zone may result from: (a) the use of inadequate or salty irrigation water, which, in conjunction with high evaporation rates and insufficient soil leaching, leads to the deposition of salts on the soil surface or in the shallow root zone (e.g., Porporato et al., 2015); (b) the presence of shallow water tables (e.g., <2.5 m deep), that allow for exfiltration of groundwater by capillary rise driven by the low soil water content at the surface (Ridolfi et al., 2008; Runyan & D'Odorico, 2010). The evaporation of exfiltrated water sustains the upward unsaturated flow through the soil column above the water table, while leading to salt at the surface (e.g., Shokri-Kuehni et al., 2020); or (c) other processes such as sea water intrusion in coastal areas (Chen & Mueller, 2018; Dasgupta et al., 2015), atmospheric deposition (dry and wet) or rock weathering (e.g., D'Odorico et al., 2013).

KHATEI ET AL. 1 of 12

Writing – original draft: Ganesh Khatei, Paolo D'Odorico, Sujith Ravi Writing – review & editing: Ganesh Khatei, Tobia Rinaldo, R. Scott Van Pelt, Paolo D'Odorico, Sujith Ravi Salt concentration in soils is often measured using electrical conductivity (EC) of the saturated soil paste extract (EC_{sp} in dS m⁻¹) and sodium absorption ratio (SAR) (e.g., Weil & Brady, 2017). Saline soils, where the exchange complex is dominated by calcium and magnesium, are characterized by EC_{sp} values greater than 4 dS m⁻¹ and SAR values less than 13. Overall, salinization of agricultural lands alters the soil's physical properties by modifying porosity, permeability, and plant-water relations (Bresler et al., 1982; Crescimanno et al., 1995; Rengasamy, 2006). Until recently, the common notion of these interactions was that soil salinity would enhance soil erosion by inducing plant mortality or at least reducing the sheltering effect of vegetation (Butcher et al., 2016; Rengasamy, 2006). Salinity-affected soils in dryland regions often experience accelerated wind erosion and represent some of the most dust emissive surfaces on Earth (Buck et al., 2011; Ravi et al., 2011). In fact, salt accumulation in the soil profile is typically related to plant stress and soil denudation (Maas & Grattan, 1999; Weil & Brady, 2017). Indeed, salts dissolved in root-zone soil reduce plant productivity through changes in soil osmotic potential and the consequent increase in plant water stress (Groenevelt et al., 2004; Sheldon et al., 2017). In these conditions plant uptake requires osmotic adjustment either through synthesis of organic solutes or through salt uptake (Sheldon et al., 2017).

While several studies have addressed the impact of soil moisture, surface roughness, soil crust, fires, grazing and agricultural practices on soil susceptibility to wind erosion, the effect of salinity still needs to be adequately explored. Previous studies on salinity's impacts on wind erosion focused mainly on the erodibility of saline hard crusts, which occur as a result of salt precipitation from solutions with high salt concentrations (Langston & McKenna Neuman, 2005; Lyles & Schrandt, 1972; Nickling, 1984; Nickling & Ecclestone, 1981). However, saline soils are more commonly found with lower salt concentrations that do not lead to the development of hard crusts (Dai et al., 2016; Li et al., 2021). Indeed, salt-affected soils often occur in intermediate states with the formation of soil aggregates and weak crusting before crust formation; in these states the presence of salt-water and the associated effect of soil aggregation is expected to affect the minimum wind velocity required for wind erosion, the "threshold velocity". The impact of these lower salt concentrations (EC_{sp} between 0.5–4 dS m⁻¹) prevalent in many agricultural areas, on soil erodibility by wind still needs to be studied. This paper investigates how the use of brackish to slightly saline irrigation water may affect soil susceptibility to wind erosion and the dust emission potential of dry soils (resembling the conditions of bare, dry agricultural soils during the dry season), and how these processes are affected by soil texture, particularly the soil clay fraction.

2. Materials and Methods

This study used a set of wind tunnel tests to detect the effect of soil salinity on the threshold velocity for wind erosion using soil samples treated with salt-enriched water at different concentrations. The same samples were also tested in another tunnel in the presence of a saltating abrader (medium sand inserted in the airstream at the bottom of the wind tunnel upstream from the soil tray) to simulate soil erosion and to sample the dust emitted by eroding soil samples under different salt treatments.

2.1. Soil Characterization and Soil Sampling

We used three agriculturally important soil types in the Southern High Plains of the United States, with a range of clay contents. The soil types used for this study are—Brownfield fine sand (BFS), Amarillo fine sandy loam (ASL), and Olton clay loam (OCL). The soil characteristics are provided in Table 1. The soils were collected from a wind erosion-affected region in the Southern High Plains (SHP) of Texas where the available irrigation water from the Ogallala Aquifer is becoming increasingly saline (Chaudhuri and Ale, 2014a, 2014b). Approximately one quarter of all irrigated farmland in the United States relies on this groundwater source (Chaudhuri & Ale, 2014b), even though the problems related to saline irrigated water are mostly limited to the SHP region. From the identified field locations, soil samples were collected from the top 5 cm, to represent the natural area exposed to the erosive action of the wind. The samples were air dried, crushed if necessary, and sieved with a 2.0 mm sieve to remove coarse debris. Clay content of the samples was determined using the standard hydrometer method (Table 1) and by laser diffraction method. The particle size analyzer (LS 13320, Beckman Coulter, Inc., CA, USA) was used to determine the size distribution of both particles suspended in a liquid (Universal Liquid Module, Beckman Coulter, Inc., CA, USA) and in air (Tornado Dry Powder System, Beckman Coulter, Inc., CA, USA). For wet dispersion, the saturated soil samples (12 hr) were dispersed in water and sonicated for 1-min before measurement to help with additional dispersion. The instrument provides a dynamic measurement range of 0.3-2,000 µm.

KHATEI ET AL. 2 of 12

Journal of Geophysical Research: Atmospheres

| Table 1 Soils Used in the Experiments | | | |
|--|----------------------|--------------------------|---------------------------------|
| Soil series (USDA soil taxonomy) | Texture (Hydrometer) | Clay (laser diffraction) | EC_{sp} (dS m ⁻¹) |
| Brownfield (BFS): Loamy, mixed, superactive, thermic Arenic Aridic Paleustalfs | Fine sand | 3% | 0.50 |
| Amarillo (ASL): Fine-loamy, mixed, superactive, thermic Aridic Paleustalfs | Sandy loam | 6% | 0.67 |
| Olton (OCL): Fine, mixed, superactive, thermic Aridic Paleustolls | Clay loam | 18% | 1.03 |

2.2. Preparing Saline Soil

The air-dried and sieved soil samples were placed in shallow trays $(77 \times 13 \times 1.6 \text{ cm}^3)$ used for the wind tunnel experiments. The trays were filled with about 2 kg of soil (slightly different amounts were needed to fill them up, depending on the soil type), packed with a roller to representative bulk densities and to match the surface of the wind tunnel floor. The trays were wetted from the bottom with deionized water and then allowed to drain to a moisture level close to field capacity, and then oven dried (60°C for 24 hr). The volume of water needed to fill the pore space to field capacity was then determined by weighing the soil tray at field capacity and after oven drying. The application of saline water with different salt concentrations (see below) was then achieved by spraying the soil surface with the (known) volume of water needed to reach field capacity using different concentrations of salt solutions. The soil trays were then allowed to drain and, again, dried at 60°C in aspirated ovens for 24 hr in order to develop structural components and a cohesive surface. To create the desired ranges of salinity, salt solutions with the target EC values were prepared by dissolving anhydrous salts in deionized water (e.g., He et al., 2013). For saline soils a mixture (by weight) of 49% CaCl₂, 41% MgCl₂, and 10% NaCl, in proportions representative of Ogallala Aquifer water chemistry was used (Hopkins, 1993; Chaudhuri and Ale, 2014a, 2014b; Haskell et al., 2022). The soil surface in each tray was allowed to equilibrate with the ambient atmospheric humidity for 1-hr before each wind tunnel test. We worked with moisture contents in equilibrium with the overlying air to avoid any soil drying during the test, which would prevent any control of surface soil moisture (Ravi et al., 2004, 2006). Soil samples were taken from the trays after the wind tunnel tests to determine the EC and SAR values (Figures S1 & S2 in Supporting Information S1).

2.3. Laboratory Wind Tunnel Experiments

Wind tunnel tests are often used to investigate the dependence of threshold velocity for wind erosion on different soil characteristics and atmospheric conditions (e.g., Mckenna-Neuman & Nickling, 1989; Ravi et al., 2006, 2006; Van Pelt et al., 2017). The measurement of threshold velocity was carried out using a non-recirculating wind tunnel at the USDA-ARS Laboratory, Big Spring, TX. The wind tunnel is 2.7 m long, 0.61 m wide, and 0.38 m high and can generate free stream velocities of 0-18.3 m s⁻¹. The test section of this wind tunnel has plexiglass windows and is equipped with removable metal trays (77 cm length, 13 cm width and 1.6 cm depth). The wind velocity was measured using a pressure transducer (Model 239, Setra, Boxborough, MA, USA) connected to a Pitot tube installed above the soil tray at 20 cm from the surface of the tunnel. The wind velocity measurements were calibrated routinely to account for the changes in the ambient air pressure and temperature (e.g., Ravi et al., 2004). Saltation (particle movement resulting from grains bouncing on the soil surface) were measured using a SENSIT flat plate movement sensor (Model FP5-RevC, Sensit Company, Redlands, CA, USA) mounted immediately downwind from the soil tray. This flat sensor, used for initiation of motion studies, has an active surface is 2.54 cm in diameter and is extremely sensitive, compared to previous versions (Sensit Company, 2013; Swann & Sherman, 2013; Poortinga et al., 2015). To remove inconsistencies in determining threshold velocity, we used the same Sensit sensor for all the wind tunnel runs. The ambient air temperature and relative humidity (Model HMP 45ASP, Vaisala, Helsinki, Finland) were also recorded. During the wind tunnel tests, the data (wind speed, air humidity and temperature and Sensit data) were collected every second (CR 23X Datalogger, Campbell Scientific Inc., Logan, UT, USA). The soils were not artificially wetted nor dried, and the variations in surface moisture content were due to changes in air humidity and temperature. All the experiments were conducted under low air humidity conditions (~20%). The soil trays were weighed before and after each run to determine soil loss rate, which was negligible (<0.1%). The wind tunnel tests consisted of four replicates of each treatment. After the initial flush out of the wind tunnel to blow away fine loose or low-density particles present on the soil surface (<1-2 min) the wind velocity was increased gradually until saltation started occurring (i.e., the Sensit started recording impact

KHATEI ET AL. 3 of 12

counts). For determining threshold velocity for wind erosion, we considered the first 10 s interval in which the Sensit recorded saltation counts for more than 50% of the time (5 out of 10 s). The maximum attainable wind velocity in the tunnel was 18 m s^{-1} . In the case of some trays no saltation conditions were ever reached, which means that in those cases the threshold velocity was greater than 18 m s^{-1} (e.g., OCL). After determining the threshold velocity, the strength of the soil surface was measured with a pocket penetrometer (H-4205, with 1-cm diameter tip, Humboldt Mfg. Co., Elgin, IL, USA). Three to four penetrometer measurements were made on each tray.

After attaining the threshold conditions, the trays were moved to another wind tunnel featuring an isokinetic total dust recovery system consisting of a hood, open at the upwind side of the soil tray and extending over the soil tray, that is connected to a series of particle settling environments by a 7.5 cm diameter aluminum tube. The particle settling environments are, in order, a 15 cm tall × 11.4 cm wide transition section with riffles in the bottom to capture saltating particles and aggregates including coarse sand followed by a large (0.325 m³ volume and 0.426 m² cross section normal to flow) settling chamber to collect medium and fine sand, and finally a housing containing two glass fiber filters (installed 'in parallel') collecting suspended sediment that is connected to the intake of a reciprocal blower. The soil trays were exposed to 20 min of wind stream at a velocity of 12.5 ms⁻¹. Saltation activity characteristic of field conditions was achieved by introducing abraders (250-350 µm clean sand) into the air stream near the ground surface of the wind tunnel and was distributed evenly across the tunnel width via chutes leading down from hopper above the tunnel. The input rate was comparable to that used in several laboratory-based wind tunnel abrasion studies (e.g., McKenna Neuman et al., 2005; Zobeck et al., 2013). After the 20-min wind tunnel run, the dust samples collected in the filters were weighed and used to determine the salt concentration. The weight of the dust samples (g) collected in the filters was divided by the weight of soil lost (g) from the corresponding trays and the test duration (minutes) to express soil loss ratio (indicator of dust emission potential) in g g⁻¹ minute⁻¹. The samples from the filter and the soil remaining in the trays were collected after the wind tunnel experiments to determine the particle size distribution and salinity.

2.4. Measuring Salinity of Soil and Dust Samples

Soil salinity was measured in terms of EC both in diluted 1:5 soil-water mixture (EC1:5) and in a saturated soil paste extract EC_{sp} (Richards, 1954). $EC_{1:5}$ was measured for soil samples collected from the trays after each wind tunnel test and for the dust samples in the filters. The EC_{sp} was measured only on a subset of soil samples, to cover the range of $EC_{1:5}$. The linear relationship found between the $EC_{1:5}$ to EC_{sp} values was then used to calculate EC_{sp} as a function of the measured $EC_{1.5}$ values (Figure S1 in Supporting Information S1). Salinity of the soil samples was determined using the Saturated Paste Extract (SPE) methodology, a commonly used technique that allows for the precise quantification of EC and SAR under controlled laboratory conditions (Rhoades et al., 1989). The air-dried soil samples were combined with deionized water and allowed to equilibrate for 24 hr to establish optimal conditions for solute migration (Rhoades et al., 1989). The amount of water required to make the saturated paste was determined experimentally considering the field capacity and soil texture. Post equilibration, the soil solutions were carefully extracted using a vacuum filtration system outfitted with a 0.45 µm filter paper for the effective separation of suspended particulates (Rhoades et al., 1989). The EC_{sp} of the extracted soil solutions were measured using a calibrated benchtop conductivity meter (PC 700, Oakton Instruments, Vernon Hills, IL). The soil extracts were then filtered through the 0.22 µm Whatman filter paper and acidified with ultra-pure nitric acid to minimize the precipitation, adsorption to the tube wall, and microbial degradation. The filtered samples were stored in the refrigerator (<4°C). An Inductively coupled plasma optical emission spectrometer (ICP-OES, iCAPTM 7600, Thermo Fisher Scientific Inc., Waltham, MA) was used to measure sodium (Na⁺), calcium (Ca²⁺), and magnesium (Mg²⁺) ion concentrations. The SAR values of the samples were calculated as:

$$SAR = \frac{Na^{+}}{\sqrt{\left[\frac{Ca^{2+} + Mg^{2+}}{2}\right]}} \tag{1}$$

where Na⁺, Ca²⁺, and Mg²⁺ are the respective ion concentrations expressed in milliequivalents per liter (mEqL⁻¹).

3. Results

The grain size analyses showed differences between wet dispersed and dry soil samples (2-mm sieved) (Figure 1), with smaller median (D_{50}) grain diameters after wet dispersion. OCL samples showed the largest decline in median grain diameter from dry to wet dispersion measurements, with 10 times decrease from 410 to 42 μ m.

KHATEI ET AL. 4 of 12

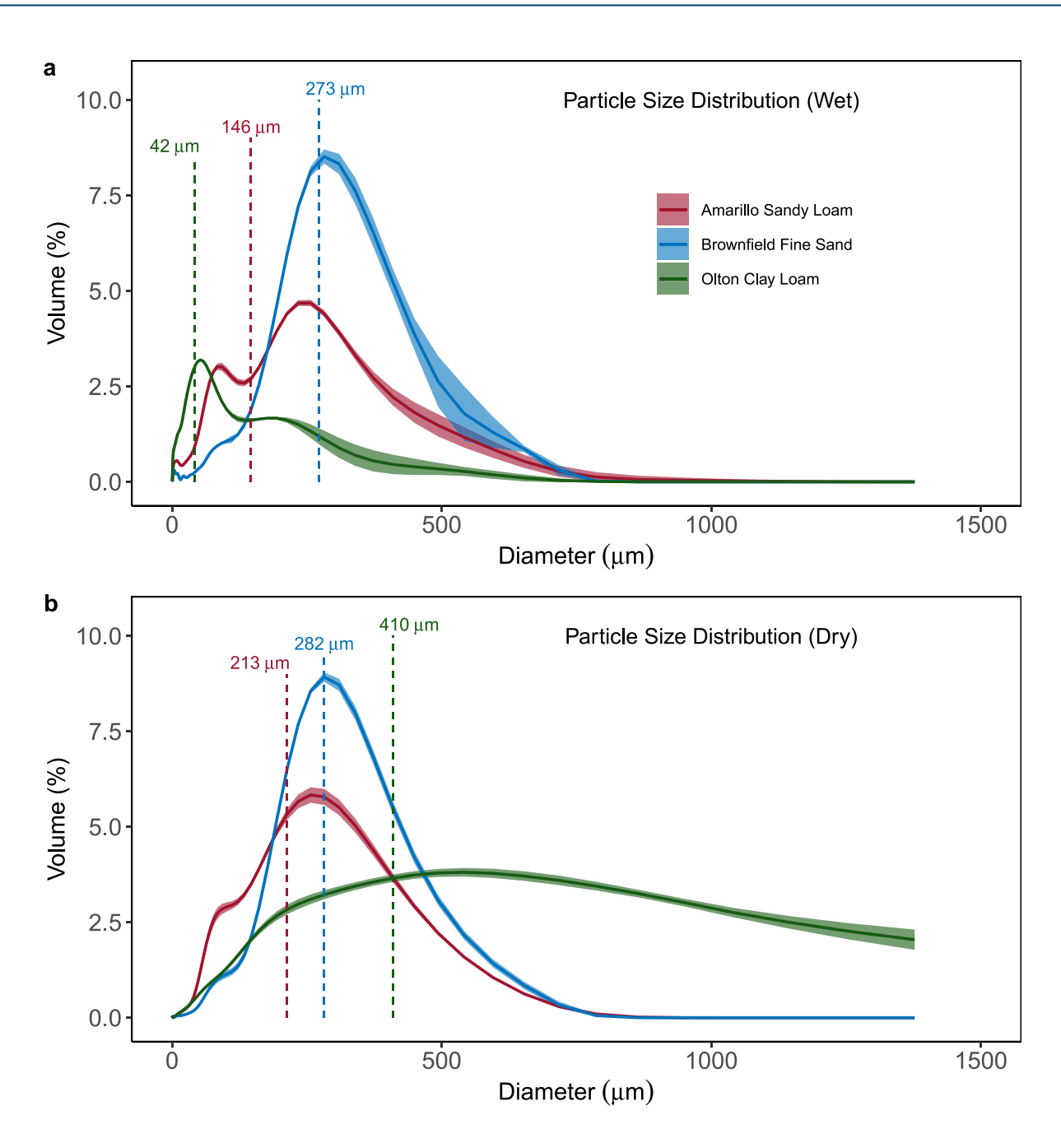


Figure 1. Particle size distribution of (a) wet and (b) dry dispersion for three soils using laser diffraction method. The vertical lines show the median value for each distribution.

We found a significant increase in threshold velocity with increasing soil salinity (EC $_{\rm sp}$) for both soils (Figure 2). Higher salinity concentrations, ranging from 0.5 to 7.0 dS m $^{-1}$ (SAR <3) correspond to an increase in threshold velocity for saltation of 100% for BFS and of 60% for ASL (see regressions in Figure 2). For both soils these relationships between threshold velocity and EC $_{\rm sp}$ were significant. The increase in threshold velocity with salinity is explained by the salt-induced formation of a soil crust, particularly with the higher concentration salt treatments. We use the micropenetrometric readings as measurements of crust strength. Interestingly, we found the crust strength increased significantly with EC $_{\rm sp}$ values (Figure 3). The relationship between average surface strength in each tray and EC $_{\rm sp}$ is significant. Threshold velocity for all the OCL treatments were found to be higher than 18.5 ms $^{-1}$, and hence it was not possible to determine the exact threshold values using this wind tunnel.

KHATEI ET AL. 5 of 12

2169896, 2024, 1, Downwaled from https://apupubs.online/harry.viely.com/oi/10.1092/203JD039576 by Ganesh Khalet - Temple University Charles Library on [03.0] 2024, See the Terms and Conditions (https://onlinelibrary.wiely.com/terms-and-conditions) on Wiley Online Library or rules of use; OA articles are governed by the applicable Cerative or [03.0] 2024, See the Terms and Conditions (https://onlinelibrary.wiely.com/terms-and-conditions) on Wiley Online Library or rules of use; OA articles are governed by the applicable Cerative or [03.0] 2024, See the Terms and Conditions (https://onlinelibrary.wiely.com/terms-and-conditions) on Wiley Online Library or rules of use; OA articles are governed by the applicable Cerative or [03.0] 2024, See the Terms and Conditions (https://onlinelibrary.wiely.com/terms-and-conditions) on Wiley Online Library or rules of use; OA articles are governed by the applicable Cerative or [03.0] 2024, See the Terms and Conditions (https://onlinelibrary.wiely.com/terms-and-conditions) on Wiley Online Library or rules of use; OA articles are governed by the applicable Cerative or [03.0] 2024, See the Terms and Conditions (https://onlinelibrary.wiely.com/terms-and-conditions) on Wiley Online Library or [03.0] 2024, See the Terms and Conditions (https://onlinelibrary.wiely.com/terms-and-conditions) on Wiley Online Library or [03.0] 2024, See the Terms and Conditions (https://onlinelibrary.wiely.com/terms-and-conditions) on Wiley Online Library or [03.0] 2024, See the Terms and Conditions (https://onlinelibrary.wiely.com/terms-and-conditions) on Wiley Online Library or [03.0] 2024, See the Terms and Conditions (https://onlinelibrary.wiely.com/terms-and-conditions) on Wiley Online Library or [03.0] 2024, See the Terms and Conditions (https://onlinelibrary.wiely.com/terms-and-conditions) on Wiley Online Library or [03.0] 2024, See the Terms and Conditions (https://onlinelibrary.wiely.com/terms-and-conditions) on Wiley Online Library or [03.0] 2024, See the Terms and Conditions (https://onlinelibra

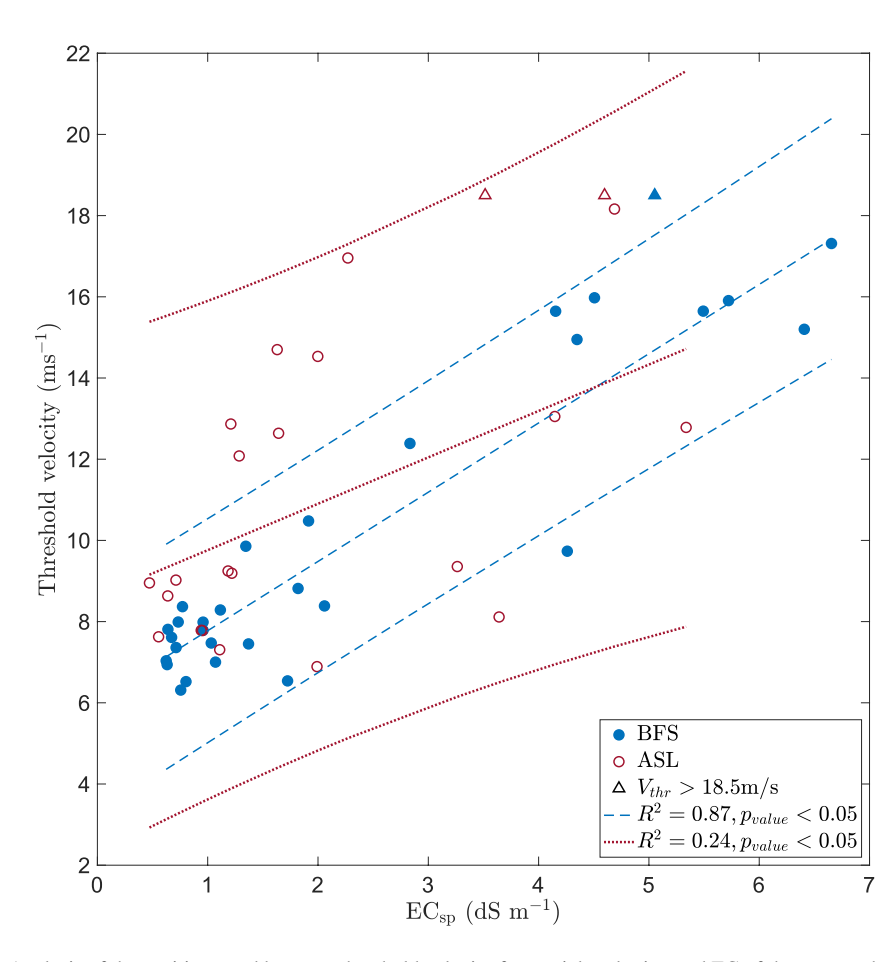


Figure 2. Analysis of the positive trend between threshold velocity for particle saltation and EC of the saturated paste extract (EC $_{\rm sp}$), that corresponds to a reduction in soil erodibility with increasing soil salinity. Each point corresponds to a different experiment run where the initial soil salinity concentration was varied. The experiments were conducted on two different soils: Brownfield fine sand (BFS—blue) and Amarillo sandy loam (ALS—red). The linear regressions of the scatter data and their corresponding 95% confidence intervals (dashed lines for BFS and dotted lines for ASL) showed that the positive nature of the relationship under investigation is significant (p-values <0.05) for both soils. In three cases no saltation occurred and, therefore, the value of 18.5 m s⁻¹ in threshold velocity (corresponding to the max attainable wind speed in the tunnel) was plotted (triangles).

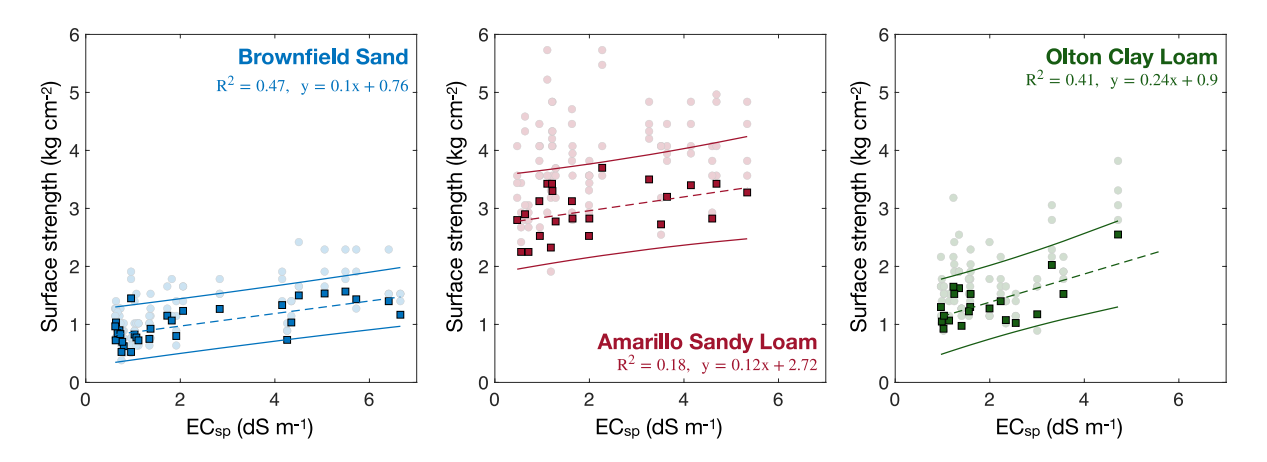


Figure 3. Micropenetrometric tests evaluated the increase in soil surface strength due to salt-induced crust formation. The positive and significant trends (dashed lines—linear regressions and solid lines—95% confidence bands) suggested that the higher surface strengths are associated with increasing soil electrical conductivity (i.e., salinity concentrations). The analysis is conducted on the averages (squares) of three to four micropenetrometric tests per tray (shaded circles).

KHATEI ET AL. 6 of 12

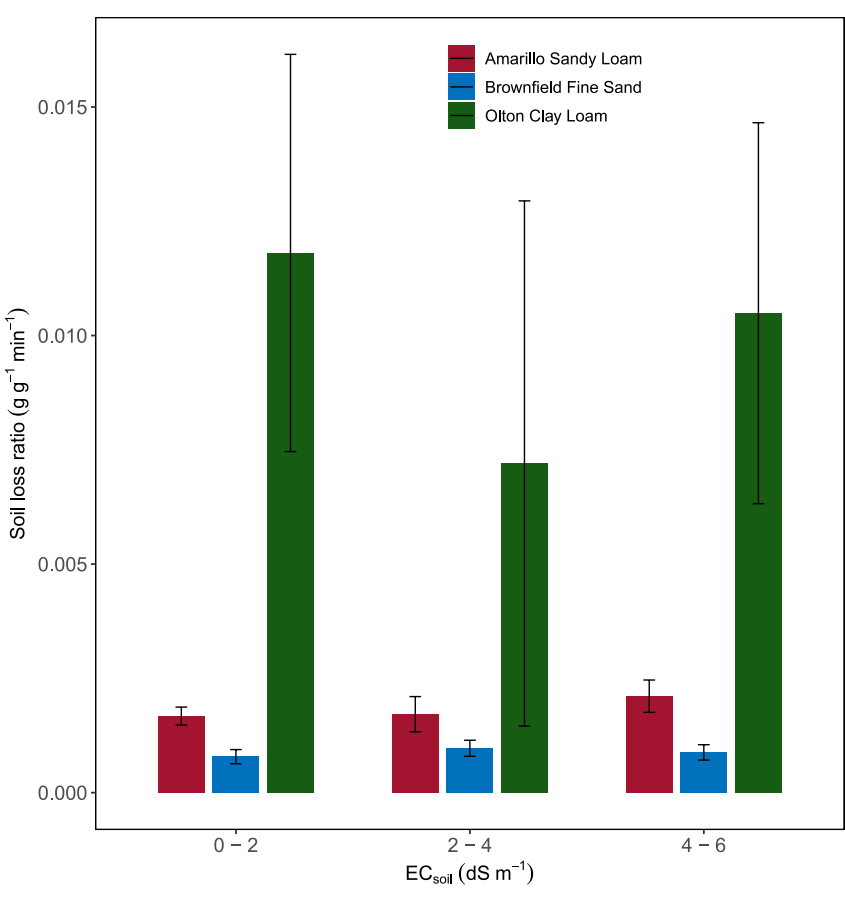


Figure 4. Dust emitted from soil samples with different salinity ranges (as represented by EC_{sp} values) as a fraction of the soil lost from the trays for the duration of each wind tunnel test.

The experiments from the second set of wind tunnel tests show that the amount of dust emitted by the soil trays - expressed both in absolute values and as a fraction of the soil lost from each tray—did not significantly change with the salt treatment (Figure 4). In the presence of an abrader, sand saltation was able to destroy the surface crust, thereby exposing the underlying soil to massive erosion independently of the salt treatment. While shorter wind tunnel experiments (i.e., <20 min duration, used in this study) are expected to be able to show differences in how quickly the soil samples are eroded in transient conditions, in the long run most of the sample is expected to be eroded. Significant differences were found to exist between the three soil types, with OCL samples emitting more dust than BFS and ASL because of the finer texture and higher clay content of the OCL samples (Table 1).

The dust emitted by the airstream in the presence of saltation had an EC_{sp} 5–10 times greater than that of the parent soil (Figure 5), suggesting that salt is preferentially emitted by air-dry soil surfaces, after the destruction of crusts. This effect is also supported by the particle size distribution of the control and saline soil, which indicate higher aggregates for OCL soil compared to other soil types (Figure 6).

4. Discussion

The mobilization and entrainment of particles from the soil surface into the airstream occurs when the wind's shear stress acting on the land surface exceeds the shear strength of the soil aggregates and their resistance to detachment. Wind speed controls the erosive action, while land surface conditions (size and shape of soil grains and aggregates, clay content, surface soil moisture, roughness, and water repellency) affect the soil erodibility, that is, the values of the threshold velocity. The finding of an increasing threshold velocity with increasing soil salinity (Figure 2) suggests that salts make soils less erodible, likely because of aggregation and the formation of a soil crust. The strength of the surface crust increases with increasing salt concentrations (Figure 3), thus suggesting that, by favoring the formation of a surface crust and enhancing its strength, salts make soils less erodible by wind.

KHATEI ET AL. 7 of 12

21698996, 2024, 1, Downloaded from https://agupubs.onlinelibrary.wiley.com/doi/10.1029/2023JD039576 by Ganesh Khatei - Temple University Charles Library

Wiley Online Library on [03/01/2024]. See the Terms

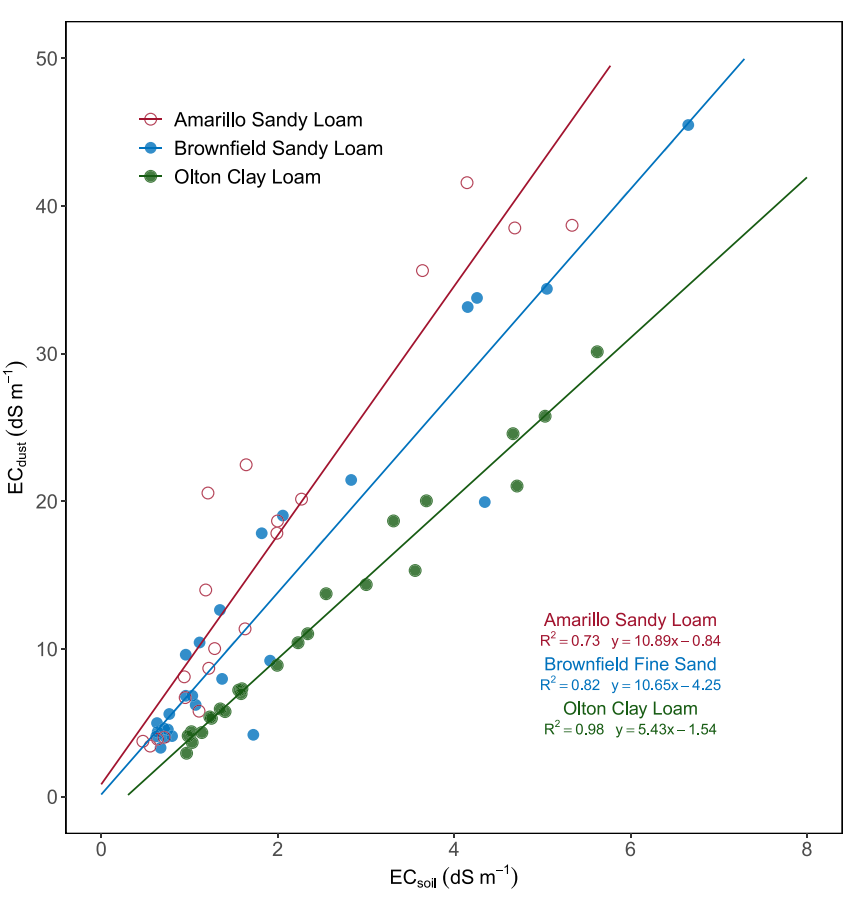


Figure 5. Relationship between salinity (EC_{sp} values) of soil and corresponding dust samples.

Moreover, crust formation and the shear strength of soil aggregates are enhanced by the clay content, as reflected by the greater threshold velocities and crust strengths found in ASL than BFS. Salt crystallization and crust development are affected by several factors including the evaporation rate, salt type and soil texture. In our study we dried the salt-treated soils at a temperature of 60°C resulting in faster evaporation rates. In fine soil particles this faster evaporation can result in finer salt crystals and a salt crust that is uniformly distributed on the soil (Dai et al., 2016; Li et al., 2021). OCL samples had lower crust strength compared to the other two soils (Figure 3) as the same amount of salt is distributed among many particles in finer OCL compared to coarse grained BFS and ASL.

Despite the salinity-induced crust strengthening effect, the second set of wind tunnel experiments shows that in the presence of a saltating abrader "bombarding" the soil crust, all soil samples get eroded regardless of the salt treatment. Similarly, no clear dependence was found between the amount of dust emitted by each sample (or the fraction of eroded sample contributing to dust emission) and the soil salt content. The salinity of the emitted dust linearly increased with the salinity of the parent soil (after salt treatment), with the former being 5–10 times more enriched than the latter. The lowest enrichment found for OCL samples compared to the other soil types can be explained by the difference in particle size distribution of dry and water dispersed soil samples (Figure 1). The OCL soil was characterized by the largest difference, reflecting the presence of clay aggregates, which contribute to a larger median grain size (410 μm) in the dry than the water dispersed samples. The medium grain size increased in saline OCL samples, indicating more aggregation (Figure 6). The applied salt can be absorbed by clays in stable aggregates, which are more resistant to erosion by wind. This effect was minimal for sandy soils, in which less aggregates were observed, resulting in enhanced erosion of salts in the emitted particulate matter. The OCL soil, due to high surface area and aggregate formation, had lower EC values compared to sandy soils, when treated with similar salt solution. Also, salinity resulted in aggregation (increase in mean particle diameter, Figure 6), where fine particles and salts are trapped in aggregates and resisted erosion even when the crust was weaker (Figure 3). Consequently, the salinity of emitted dust was only 5 times higher than the background soil for OCL, while it was 10 times higher for sandy soils.

KHATEI ET AL. 8 of 12

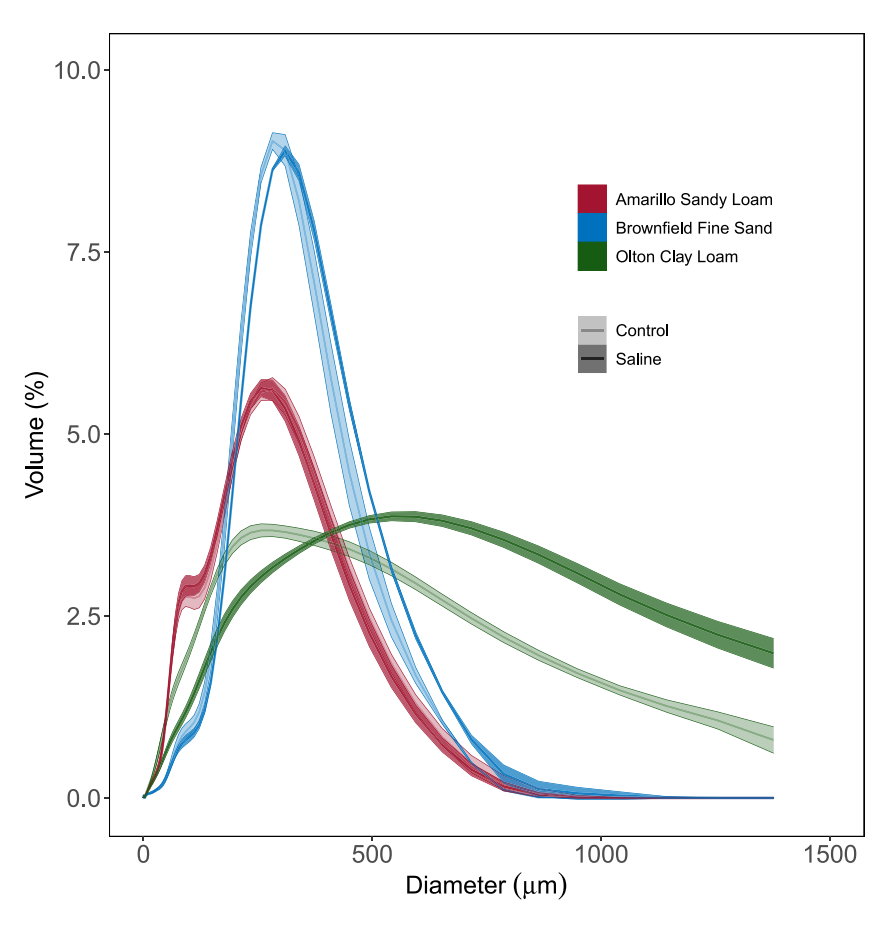


Figure 6. Particle size distribution for the control and saline (EC_{sp} \sim 4 dS m⁻¹) soils using laser diffraction method (dry dispersion).

Airborne salt can be either in the form of dust-sized salt crystals or bonded to mineral dust. The larger salt concentration in the dust than in the parent soil can be explained by the fact that dust is largely contributed by clay minerals, which are known for their relatively high cation exchange capacity. Further, salt particles, as those used in the study (CaCl₂, MgCl₂, and NaCl) have lower density ranges of 2,150–2,320 kg m⁻³, compared to bulk soil particles, which varies between 2,550 and 2,700 kg m⁻³. Salt particles can be preferentially entrained by wind, even before the characteristic threshold condition for the soil is attained. Post-threshold conditions, the dominant particulate matter emission mechanism is the surface abrasion by saltating sand particles (Baddock et al., 2013; Shao et al., 1993). The particle emission by abrasion is shown to depend on several factors including the saltation flux, velocity of the abrader, impact angle and the properties of the target surfaces including the crushing energy of aggregates or particles (Pi et al., 2020). As salt particles are characterized by lower particle density and load-bearing capacity, the crushing energy of salt particles (and modulus of rupture) is much lower than typical soil particles. So saltating sand particles colliding with salt crystals can disintegrate them more efficiently than soil particles and generate fine particles (Figure 7a). To demonstrate the effect of density and particle size on threshold shear velocity for dry soil and salt particles, we adopted a semi-empirical expression for the saltation fluid threshold (Shao & Lu, 2000). Even though the parameters are not derived from our experiments and the threshold velocity also depends on other factors including particle size, shape, aggregates, moisture, it is instructive to visualize the effect of density and particle size on threshold shear velocity for dry soil and salt particles (Figure 7b).

$$u_{*t} = A_N \sqrt{\frac{\rho_p - \rho_a}{\rho_a} g D_p + \frac{\gamma}{\rho_a D_p}}$$
 (2)

where the ρ_a is the air density, ρ_p is the particle density, D_p is the particle diameter, g is the acceleration due to gravity, $A_N = 0.11$ is a dimensionless parameter, γ is a parameter which scales the strength of the interparticle forces. Here we use $\gamma = 2.9 \times 10^{-4} \, \mathrm{Nm^{-1}}$ from Kok and Renno (2006) for air-dry loose soil particles.

KHATEI ET AL. 9 of 12

21 69896, 2024. 1, Downloaded from https://agupubs.onlinelibrary.wiley.com/doi/10.1029/2023JD039576 by Ganesh Khaei - Temple University Charles Library - Wiley Online Library on [03/01/2024]. See the Terms and Conditions (https://agupubs.onlinelibrary.wiley.com/doi/10.1029/2023JD039576 by Ganesh Khaei - Temple University Charles Library - Wiley Online Library on [03/01/2024]. See the Terms and Conditions (https://agupubs.onlinelibrary.wiley.com/doi/10.1029/2023JD039576 by Ganesh Khaei - Temple University Charles Library - Wiley Online Library on [03/01/2024]. See the Terms and Conditions (https://agupubs.onlinelibrary.wiley.com/doi/10.1029/2023JD039576 by Ganesh Khaei - Temple University Charles Library - Wiley Online Library on [03/01/2024]. See the Terms and Conditions (https://agupubs.onlinelibrary.wiley.com/doi/10.1029/2023JD039576 by Ganesh Khaei - Temple University Charles Library - Wiley Online Library on [03/01/2024]. See the Terms and Conditions (https://agupubs.onlinelibrary.wiley.com/doi/10.1029/2023JD039576 by Ganesh Khaei - Temple University Charles Library - Wiley Online Library on [03/01/2024]. See the Terms and Conditions (https://agupubs.onlinelibrary.wiley.com/doi/10.1029/2023JD039576 by Ganesh Khaei - Temple University Charles Library - Wiley Online Library on [03/01/2024]. See the Terms and Conditions (https://agupubs.onlinelibrary.wiley.com/doi/10.1029/2023JD039576 by Ganesh Khaei - Temple University Charles Library - Wiley Online Library - Wiley On

Figure 7. (a) A schematic representation of two-dimensional eolian erosion and transport processes with soil and salt particles on a salt crusted surface. (b) Theoretical threshold shear velocity for initiating saltation for soil and salt particles calculated with different size and density ranges. The shaded region indicates density ranges for salts used in the experiment $(CaCl_2, MgCl_2, and NaCl, 2.15-2.32 \text{ g cm}^{-3})$ and bulk soil particles $(2.55-2.70 \text{ g cm}^{-3})$.

Even though salinity increased the resistance to wind erosion in the early stages, the negative impacts of salinity on soil quality and crop productivity needs to be considered (Rengasamy, 2006). Soil salinization can enhance wind erosion by inducing plant mortality or at least reducing the sheltering effect of vegetation, a dominant control on wind erosion in drylands (Butcher et al., 2016; Rengasamy, 2006). Moreover, the salt aggregates and crusts were readily ruptured by saltating sand grains resulting in comparable or sometimes even higher particulate matter emissions compared to non-saline soils. Salt crusts are found to break down and erode in response to sustained abrasion in natural environments, resulting in emission of fine aerosols with impact on air quality and human health (Cahill et al., 1996; Langston & McKenna Neuman, 2005). Our results also show that the emitted dust aerosols contained a disproportionate amount of salts compared to the background soil. OCL, with higher clay content, had lower concentration of salts in the emitted sediments compared to BFS and ASL. In OCL soil the salt might be adsorbed on stable clay aggregates in the soil, which resist erosion. The preferential entrainment of salts, in the form of minute salt crystals or salt ions bound to mineral dust, may impact salinization

KHATEI ET AL. 10 of 12

of other soils in the region and the spread of contaminants from agricultural areas (Gill et al., 2002; Goldstein et al., 2017). Even though most toxic contaminants in the soil are retained in the vadose zone resulting in lower concentrations in the surface salt crusts, anthropogenic disturbances to soil (agricultural activities) can result in translocation of contaminants to surface soils (Goldstein et al., 2017).

5. Conclusions

Our study shows an initial reduction in wind erosion with increasing soil salinity, as reflected by the increase in threshold velocity associated with salt-induced soil aggregation and crust formation. However, in the presence of an abrader the soil crust is disintegrated by saltation, which breaks the crust, thus leading to even higher dust emissions, than in the control samples. Interestingly, we found an increase in salt content in emitted dust with respect to the "parent soil", which suggests that salt and dust particles with attached salt are preferentially removed from the soil by the air flow (in fact the EC of particulates were almost 10 times greater than the EC of the parent soil samples). The subsequent deposition of airborne salt onto adjacent land may lead to the salinization of nearby (downwind) areas. Moreover, salts can serve as vectors of airborne contaminants, which are expected to be easily soluble once inhaled. Thus, the higher salt concentration found in the dust than in the soil suggests that either minuscule dust crystals or salt ions bound to mineral dust get preferentially entrained in the airflow, thus favoring the airborne transport of salts with important effect on the salinization of other soils in the region and the spread of pathogen and respiratory diseases.

Conflict of Interest

The authors declare no conflicts of interest relevant to this study.

Data Availability Statement

All data used in our work can be found online Khatei et al. (2023) (https://figshare.com/s/57e44668eeff66081fed).

References

Baddock, M., Boskovic, L., Strong, C., McTainsh, G., Bullard, J., Agranovski, I., & Cropp, R. (2013). Iron-rich nanoparticles formed by Aeolian abrasion of desert dune sand. *Geochemistry, Geophysics, Geosystems*, 14(9), 3720–3729. https://doi.org/10.1002/ggge.20229

Bresler, E., McNeal, B. L., & Carter, D. L. (1982). Saline and sodic soils. Advanced Series in Agricultural Sciences, 10. https://doi.org/10.1007/978-3-642-68324-4

Buck, B. J., King, J., & Etyemezian, V. (2011). Effects of dust emissions, Salton sea, California. Soil Science Society of America Journal, 75(5), 1971–1985. https://doi.org/10.2136/sssai2011.0049

Butcher, K., Wick, A. F., DeSutter, T., Chatterjee, A., & Harmon, J. (2016). Soil salinity: A threat to global food security. *Agronomy Journal*, 108(6), 2189–2200. https://doi.org/10.2134/agroni2016.06.0368

Cahill, T. A., Gill, T. E., Reid, J. S., Gearhart, E. A., & Gillettee, D. A. (1996). Saltating particles, playa crusts and dust aerosols at Owens (dry) lake, California. Earth Surface Processes and Landforms, 21(7), 621–639. https://doi.org/10.1002/(sici)1096-9837(199607)21:7<621::aid-esp661>3.0.co;2-e

Chaudhuri, S., & Ale, S. (2014a). Temporal evolution of depth-stratified groundwater salinity in municipal wells in the major aquifers in Texas, USA. Science of the Total Environment, 472, 370–380. https://doi.org/10.1016/j.scitotenv.2013.10.120

Chaudhuri, S., & Ale, S. (2014b). Long-term (1960–2010) trends in groundwater contamination and salinization in the Ogallala aquifer in Texas. Journal of Hydrology, 513, 376–390. https://doi.org/10.1016/j.jhydrol.2014.03.033

Chen, J., & Mueller, V. (2018). Coastal climate change, soil salinity and human migration in Bangladesh. *Nature Climate Change*, 8(11), 981–985. https://doi.org/10.1038/s41558-018-0313-8

Crescimanno, G., Iovino, M., & Provenzano, G. (1995). Influence of salinity and sodicity on soil structural and hydraulic characteristics. *Soil Science Society of America Journal*, 59(6), 1701–1708. https://doi.org/10.2136/sssaj1995.03615995005900060028x

Dai, S., Shin, H., & Santamarina, J. C. (2016). Formation and development of salt crusts on soil surfaces. *Acta Geotechnica*, 11(5), 1103–1109. https://doi.org/10.1007/s11440-015-0421-9

Dasgupta, S., Hossain, M. M., Huq, M., & Wheeler, D. (2015). Climate change and soil salinity: The case of coastal Bangladesh. *Ambio*, 44(8), 815–826. https://doi.org/10.1007/s13280-015-0681-5

D'Odorico, P., Bhattachan, A., Davis, K. F., Ravi, S., & Runyan, C. W. (2013). Global desertification: Drivers and feedbacks. *Advances in Water Resources*, 51, 326–344. https://doi.org/10.1016/j.advwatres.2012.01.013

Gill, T. E., Gillette, D. A., Niemeyer, T., & Winn, R. T. (2002). Elemental geochemistry of wind-erodible playa sediments, Owens Lake, California. Nuclear Instruments and Methods in Physics Research Section B: Beam Interactions with Materials and Atoms, 189(1), 209–213. https://doi.org/10.1016/S0168-583X(01)01044-8

Goldstein, H. L., Breit, G. N., & Reynolds, R. L. (2017). Controls on the chemical composition of saline surface crusts and emitted dust from a wet playa in the Mojave Desert (USA). *Journal of Arid Environments*, 140, 50–66. https://doi.org/10.1016/j.jaridenv.2017.01.010

Groenevelt, P. H., Grant, C. D., & Murray, R. S. (2004). On water availability in saline soils. Soil Research, 42(7), 833-840. https://doi.org/10.1071/SR03054

Haskell, D., Heo, J., Park, J., & Dong, C. (2022). Hydrogeochemical evaluation of groundwater quality parameters for Ogallala aquifer in the Southern high plains region, USA. *International Journal of Environmental Research and Public Health*, 11 19(14), 8453. https://doi. org/10.3390/ijerph19148453

Acknowledgments

This research was funded by the U.S. National Science Foundation (NSF) Award EAR#2054170 for S. Ravi, Award EAR#2053857 for P. D'Odorico.

KHATEI ET AL. 11 of 12

21698996, 2024, 1, Downloaded

- Hassani, A., Azapagic, A., & Shokri, N. (2020). Predicting long-term dynamics of soil salinity and sodicity on a global scale. Proceedings of the National Academy of Sciences, 117(52), 33017–33027. https://doi.org/10.1073/pnas.2013771117
- He, Y., DeSutter, T. M., & Clay, D. E. (2013). Dispersion of pure clay minerals as influenced by calcium/magnesium ratios, sodium adsorption ratio, and electrical conductivity. Soil Science Society of America Journal, 77(6), 2014–2019. https://doi.org/10.2136/sssaj2013.05.0206n
- Hopkins, J. (1993). Water-quality evaluation of the Ogallala aquifer, Texas. Texas Water Development Board. Report 342.
- Khatei, G., Rinaldo, T., Van Pelt, S., D'Odorico, P., & Ravi, S. (2023). Salinity_project [Dataset]. figshare. https://figshare.com/s/57e44668eeff66081fed
- Kok, J. F., & Renno, N. O. (2006). Enhancement of the emission of mineral dust aerosols by electric forces. Geophysical Research Letters, 33(19). https://doi.org/10.1029/2006g1026284
- Langston, G., & McKenna Neuman, C. (2005). An experimental study on the susceptibility of crusted surfaces to wind erosion: A comparison of the strength properties of biotic and salt crusts. *Geomorphology*, 72(1), 40–53. https://doi.org/10.1016/j.geomorph.2005.05.003
- Li, S., Li, C., & Fu, X. (2021). Characteristics of soil salt crust formed by mixing calcium chloride with sodium sulfate and the possibility of inhibiting wind-sand flow. Scientific Reports, 11(1), 9746. https://doi.org/10.1038/s41598-021-89151-1
- Lyles, L., & Schrandt, R. L. (1972). Wind erodibility as influenced by rainfall and soil salinity. Soil Science, 114(5), 367–372. https://doi.org/10.1097/00010694-197211000-00007
- Maas, E. V., & Grattan, S. R. (1999). Crop yields as affected by salinity. Agricultural Drainage, 55–108. https://doi.org/10.2134/agronmonogr38.c3
 McKenna Neuman, C., Maxwell, C., & Rutledge, C. (2005). Spatial and temporal analysis of crust deterioration under particle impact. Journal of Arid Environments, 60(2), 321–342. https://doi.org/10.1016/j.jaridenv.2004.04.007
- Mckenna-Neuman, C., & Nickling, W. G. (1989). A theoretical and wind tunnel investigation of the effect of capillary water on the entrainment of sediment by wind. Canadian Journal of Soil Science, 69(1), 79–96. https://doi.org/10.4141/cjss89-008
- Nickling, W. G. (1984). The stabilizing role of bonding agents on the entrainment of sediment by wind. Sedimentology, 31(1), 111–117. https://doi.org/10.1111/j.1365-3091.1984.ib00726.x
- Nickling, W. G., & Ecclestone, M. (1981). The effects of soluble salts on the threshold shear velocity of fine sand. Sedimentology, 28(4), 505–510. https://doi.org/10.1111/j.1365-3091.1981.tb01698.x
- Pi, H., Huggins, D. R., Webb, N. P., & Sharratt, B. (2020). Comparison of soil-aggregate crushing-energy meters. *Aeolian Research*, 42, 100559. https://doi.org/10.1016/j.aeolia.2019.100559
- Poortinga, A., Van Rheenen, H., Ellis, J. T., & Sherman, D. J. (2015). Measuring Aeolian sand transport using acoustic sensors. *Aeolian Research*, 16, 143–151. https://doi.org/10.1016/j.aeolia.2014.12.003
- Porporato, A., Feng, X., Manzoni, S., Mau, Y., Parolari, A. J., & Vico, G. (2015). Ecohydrological modeling in agroecosystems: Examples and challenges. *Water Resources Research*, 51(7), 5081–5099. https://doi.org/10.1002/2015WR017289
- Ravi, S., D'Odorico, P., Breshears, D. D., Field, J. P., Goudie, A. S., Huxman, T. E., et al. (2011). Aeolian processes and the biosphere. *Reviews*
- of Geophysics, 49(3). https://doi.org/10.1029/2010RG000328
 Ravi, S., D'Odorico, P., Over, T. M. T. M., & Zobeck, T. M. T. M. (2004). On the effect of air humidity on soil susceptibility to wind erosion: The
- case of air-dry soils. Geophysical Research Letters, 31(9). https://doi.org/10.1029/2004GL019485

 Rayi S, Zobeck T M, Over T M, Okin G S, & D'Odorico P (2006). On the effect of moisture bonding forces in air-dry soils on threshold
- Ravi, S., Zobeck, T. M., Over, T. M., Okin, G. S., & D'Odorico, P. (2006). On the effect of moisture bonding forces in air-dry soils on threshold friction velocity of wind erosion. Sedimentology, 53(3), 597–609. https://doi.org/10.1111/j.1365-3091.2006.00775.x
- Rengasamy, P. (2006). World salinization with emphasis on Australia. Journal of Experimental Botany, 57(5), 1017–1023. https://doi.org/10.1093/ivb/eri108
- Rhoades, J. D., Manteghi, N. A., Shouse, P. J., & Alves, W. J. (1989). Estimating soil salinity from saturated soil-paste electrical conductivity. *Soil Science Society of America Journal*, 53(2). https://doi.org/10.2136/sssaj1989.03615995005300020067x
- Richards, L. A. (1954). Diagnosis and improvement of saline and alkali soils. Soil Science, 78(2), 154. https://doi.org/10.1097/00010694-195408000-00012
- Ridolfi, L., Laio, F., & Odorico, P. D. (2008). Fertility island formation and evolution in dryland ecosystems. *Ecology and Society*, 13(1), 5. https://doi.org/10.5751/ES-02302-130105
- Runyan, C. W., & D'Odorico, P. (2010). Ecohydrological feedbacks between salt accumulation and vegetation dynamics: Role of vegetation-groundwater interactions. Water Resources Research, 46(11), https://doi.org/10.1029/2010WR009464
- Sensit Company. (2013). Movement detector. Technical manual-Model FP5-RevC. Sensit company.
- Shahid, S. A., Zaman, M., & Heng, L. (2018). Soil salinity: Historical perspectives and a world overview of the problem. In *Guideline for salinity assessment, mitigation and adaptation using nuclear and related techniques*. Springer. https://doi.org/10.1007/978-3-319-96190-3_2
- Shao, Y., & Lu, H. (2000). A simple expression for wind erosion threshold friction velocity. *Journal of Geophysical Research*, 105(D17), 22437–22443. https://doi.org/10.1029/2000JD900304
- Shao, Y., Raupach, M. R., & Findlater, P. A. (1993). Effect of saltation bombardment on the entrainment of dust by wind. *Journal of Geophysical Research*, 98, 12712–12726. https://doi.org/10.1029/93JD00396
- Sheldon, A. R., Dalal, R. C., Kirchhof, G., Kopittke, P. M., & Menzies, N. W. (2017). The effect of salinity on plant-available water. *Plant and Soil*, 418(1), 477–491. https://doi.org/10.1007/s11104-017-3309-7
- Shokri-Kuehni, S. M. S., Raaijmakers, B., Kurz, T., Or, D., Helmig, R., & Shokri, N. (2020). Water table depth and soil salinization: From pore-scale processes to field-scale responses. *Water Resources Research*, 56(2), e2019WR026707. https://doi.org/10.1029/2019WR026707
- Swann, C., & Sherman, D. J. (2013). A bedload trap for Aeolian sand transport. Aeolian Research, 11, 61–66. https://doi.org/10.1016/j.aeolia.2013.09.003
- Szabolcs, I. (1989). Salt-affected soils. CRC Press.
- Van Pelt, S., Baddock, M., Zobeck, T. M., Ravi, S., D'Odorico, P., & Bhattachan, A. (2017). Total vertical sediment flux and PM₁₀ emissions from disturbed Chihuahuan Desert surfaces. *Geoderma*, 293, 19–25. https://doi.org/10.1016/j.geoderma.2017.01.031
- Weil, R. R., & Brady, N. C. (2017). The nature and properties of soils. Pearson Press.
- Zobeck, T. M., Baddock, M., Scott Van Pelt, R., Tatarko, J., & Acosta-Martinez, V. (2013). Soil property effects on wind erosion of organic soils. Aeolian Research, 10, 43–51. https://doi.org/10.1016/j.aeolia.2012.10.005

KHATEI ET AL. 12 of 12